

A 3.9 MeV Photoinjector and Delay System for Wakefield Measurements

J. G. Power, M. E. Conde

Argonne National Laboratory

9700 S. Cass Ave Argonne IL, 60439

ABSTRACT

We report on the characterization of the 3.9 MeV electron beam from an rf photoinjector at the Argonne Wakefield Accelerator. This beam is used to diagnose wakefields produced by the 15 MeV beam from a second rf photoinjector. We measured the emittance with the usual quadrupole scan method but using a new fitting algorithm that includes space charge forces. This photocathode gun has produced a beam charge per pulse ranging from 10 pC to 4 nC, but is normally operated at 100 pC with a measured normalized emittance of 3.4π mm mrad and bunch length of 8 ps FWHM.

PACS: 41.75.Lx, 41.75.Fr, 41.85.E

*Accepted for publication in the **Review of Scientific Instruments** in the **Article** Section

I Introduction

New particle acceleration techniques using wakefields excited by electron beams have been under intense investigation in the last 10 years¹. The method by which wakefield acceleration² can be used as the technology for future accelerators is easy to understand. A high charge “drive” beam passes through a structure (or plasma) and excites a strong longitudinal wakefield capable of accelerating a trailing “witness” beam. To investigate this scheme, we map the wakefield out by observing the change in energy of the witness beam as a function of delay behind the drive beam. Therefore, to perform wakefield experiments, one needs to do three things: generate a drive beam, generate a witness beam, and develop a delay system to control the separation between the two beams. The early wakefield acceleration experiments performed at the Advanced Accelerator Test Facility³ (AATF) used a single thermionic electron gun to produce both the drive and witness beams. Controlling the time separation between the beams was an arduous task since one had to first split the original electron beam in two and then send the witness electron beam into a magnetic transport line of variable length that was under vacuum. In this paper we describe the current wakefield acceleration experiment at the Argonne Wakefield Accelerator (AWA), the delay system and then present the measurements made to characterize the witness beam.

II AWA Facility and Delay System Description

The wakefield experiment⁴ currently underway at the AWA employs separate L-band, rf photocathode guns to create the drive and witness beams. Having two guns allows us to control the time separation between the beams in a much simpler fashion at the AWA compared with the AATF. The variable delay laser system shown in FIG. 1. delays the laser light to the witness rf photocathode gun⁵ relative to the drive photocathode gun. The power splitter diverts 15% of the laser beam (248 nm, 2-5 mJ) into a retro-reflector located on a movable translation stage which produces a maximum optical path length change of 1 m. The translation stage is controlled by a stepping motor with a minimum increment of 10 μm (33 fs). At the exit of this system, the two beams emerge with a vertical separation of 0.5 inch. This separation allows one to use mirrors to direct the two beams into their respective guns.

Figure. 2. shows a simplified block diagram of the AWA. The drive gun^{4,6} is optimized for both low power consumption (1.5 MW) by utilizing a 1/2 cell, high Q geometry and high charge by using magnesium as the photocathode material. Two L-band linac tanks⁷ accelerate the 1.5 MeV drive beam from the gun, to an energy of 15 MeV for injection into the transport line. We introduce a magnetic chicane in the drive line so we can combine the two beams with Combination Dipole. The witness beam is steered toward Combination Dipole when Witness Dipole is energized. After emerging from the combination dipole, the drive and witness beams each move through the center of the wakefield device sepa-

rated by a distance determined by the variable delay system. The drive beam generates wakefields as it passes through the wakefield device. We map out the wake potential by measuring the change in energy of the trailing witness beam as a function of delay behind the drive beam using the magnetic spectrometer (round dipole on the right side of FIG. 2).

A good probe for our wakefield measurement system is well separated from the drive beam in energy (so it is easy to resolve in the spectrometer), 10 ps or less in duration, 1% energy spread, and low charge (100 pC) compared to the drive beam. Since this parameter list is easy to achieve with a photocathode gun, we chose the witness gun design with simplicity in mind. The witness gun design is essentially a section of the SLAC MARK III⁸ S-band accelerating structure scaled to L-band. Figure. 3. shows a SUPERFISH⁹ simulation of the 6 cell, $\pi/2$ photocathode gun with radius $a = 2.5$ cm and radius $b = 9.08$ cm. We chose the $\pi/2$ mode because it is relatively easy to work with electrically due to the wide mode separation. For 3.8 MW of rf power, PARMELA¹⁰ simulations show the witness gun produces a 4 MeV, 100 pC beam with a FW energy spread of 0.75% and an emittance of 1.9 mm mrad.

III Witness Beam Characterization

The experimental setup for witness beam diagnostics is also shown in FIG. 2. The charge is measured immediately after the witness gun with an integrating current transformer (ICT) from Bergoz (model ICT-082-070-10:1). We

measured bunch charges from 10 pC to 4 nC at the ICT, but all the measurements presented in this paper are for bunches of 100 pC which is the nominal operating charge for wakefield measurements. Energy and energy spread measurements were made with the spectrometer (6 inch diameter, resolution 1.0 %) at the end of the beamline (the round-pole magnet labeled D at the rightmost of FIG. 2). All energy and energy spread measurements were made with the wakefield device removed from the beamline so as not to interfere with the measurements. For 4 MW of rf power into the witness gun we measured a beam energy of 3.85 MeV using. We only measured an upper limit for the energy spread (1.6 %) since at the time of the measurement there was no quadrupole in front of the spectrometer.

To make bunch length or emittance measurements, the witness dipole (FIG. 2) is not energized so that the beam propagates into the diagnostic port. For bunch length measurements, a 1 mm thick quartz plate is inserted into the beam path to produce Cherenkov light. This light is then imaged onto the slit of a streak camera (Hamamatsu, model C1587, 1.6 ps resolution). Figure 4 shows a typical streak camera image of the cherenkov light produced by the witness beam. The FWHM of the beam is 34 channels or 11 ps. We obtained an average FWHM of 8 ps for the witness beam pulse length. Unlike emittance and energy spread, bunch length is extremely sensitive to the launch phase angle in the gun. Based on our energy measurements ($E = 3.9$ MeV, $\Delta E/E = 1.0$ %) we know that

the launch phase was between 20° and 60° which corresponds to a predicted bunch length of 3.5 ps and 9.0 ps respectively from the PARMELA simulation. This shows that the measurement is within the bounds of the simulation.

We measured the emittance with the quad scan technique where the beam spot size is measured as a function of quadrupole strength. In our case, the beam spot size is measured on a phosphor screen in Diagnostic Chamber of FIG. 2 as a function of current in the quadrupole labeled Quad Scan. The beam spot on the phosphor is digitized with a camera and frame grabber from Imaging Technology (MVC 150/40-VME) and saved for off-line analysis. Space charge forces dominate the transport of the beam at 100 pC, since the energy of the beam is only 3.85 MeV. Therefore, we developed a new fitting algorithm that takes space charge forces into account as explained below.

The rms. beam envelope¹¹, R , of a round beam evolves along the beam propagation axis (s -axis) according to

$$R''(s) = \frac{\epsilon^2}{R^3(s)} + \frac{K}{R(s)} \quad (1)$$

where the derivative is taken with respect to s , ϵ is the emittance, and K , the perveance¹² in vacuum, is

$$K = \frac{I}{I_0} \frac{2}{\beta^3 \gamma^3} \quad (2)$$

where I is the beam current and I_0 is the Alfven current equal to 17 kA. As op-

posed to other quad scans, we keep both terms in (1) for our fit of the data. We then fit the data to (1) with a non-linear least squares Mathematica¹² program

In order to study the new quad scan fitting algorithm, we generated test data sets with the simulation code TRACE 3D. We used TRACE 3D instead of PARMELA since PARMELA runs slower on a computer. TRACE 3D solves for the rms beam envelope in the x, y and z directions, including linear space-charge forces. On the other hand, PARMELA is a particle pushing code, including complete space-charge forces, capable of tracking 50,000 particles through a set of external fields. Since TRACE 3D only solves for the envelope it can be run quickly over a large set of parameters.

For a particular test case¹³ similar to the witness beam (100 pC & 10 ps) the quad scan fitting algorithm without space charge overestimates the emittance by 90 % while the algorithm including space charge reproduces the data to within 16% of the simulated data. In the case of an emittance measurement from a photocathode gun at such low energies (3.9 MeV) an agreement of 16% is considered excellent. The reason that the fit does not duplicate the emittance number from the TRACE 3D simulation is TRACE 3D is fully 3 dimensional while the model is only 1D. It may be possible to improve the algorithm further by solving the more computer intensive coupled beam equations¹¹

$$X''(s) = \frac{\epsilon_x^2}{X^3(s)} + \frac{2K}{X(s) + Y(s)} \quad (3)$$

$$Y''(s) = \frac{\epsilon_y^2}{Y^3(s)} + \frac{2K}{X(s) + Y(s)} \quad (4)$$

where $X(s)$ and $Y(s)$ are the boundaries of the beam envelope and ϵ_x and ϵ_y are the x and y emittances. Since the agreement with data using the round beam approximation is suitable for our purposes we will not extend the model here.

Using the quad scan technique based on (1) we measured a normalized emittance of 3.4π mm mrad. The geometrical emittance is $3.4/\beta\gamma = 0.41$ mm mrad as shown in FIG. 5. The scattering in the data is due to charge fluctuation during the data acquisition. The discrepancy between the experimentally measured emittance of 3.4 mm mrad and the predicted emittance from PARMELA of 1.9 mm mrad is considered to be acceptable for a photocathode gun. That said, we can still examine the sources of error. These come mainly from the limitations of the imaging system and assumptions about the beam's profile. Both the phosphor screen and camera may not be linear over the range we used it and the frame grabber has a dynamic range of only 8 bits. We assumed a gaussian beam profile to calculate the rms spot size from the FWHM data. Since we observed that the beam profile is not a true gaussian, our results are only approximately true. This fitting algorithm not only works for quad scans, but any measurement technique in which the beam is transported under space charge dominated conditions.

IV Summary

The end result of this work is a functioning wakefield measurement sys-

tem that has been used to measure the first wakefields produced at the AWA. The rf photocathode gun used to generate the witness beam has produced an electron beam with an energy of 3.9 MeV, a charge of 100 pC, a normalized transverse emittance of 3.4π mm mrad, and a FWHM bunch length of 8 ps. The beam characterization is found to agree well with the predictions based on the SUPERFISH and PARMELA simulations.

The authors would like to thank E. Chojnacki, W. Gai, R. Konecny, P. Schoessow, and J. Simpson. This work was supported by the U.S. Department of Energy, Division of High Energy Physics, Contract No. W-31-109-ENG-38

REFERENCES

1. For example: the Advanced Accelerator Workshop conference proceedings, edited by P. Schoessow, AIP-335 (Fontana, Wi, 1994)
2. R. Keinigs, M. Jones and W. Gai, Part. Accel, **24**, 223 (1989)
3. W. Gai, P. Schoessow, B. Cole, R. Konecny, J. Norem J. Rosezweig and J. Simpson, Phys. Rev. Lett. **61**, No. 24, 2756 (1988)
4. P. Schoessow, E. Chojnacki, W. Gai, C. Ho, R. Konecny, J. G. Power, M. Rosing, J. Simpson, N. Barov and M.E. Conde, Particle Accelerator Conference and International Conference on High-Energy Accelerators, pg. 976, (Dallas, Tx, 1995)
5. J. G. Power, Ph.D. Thesis , Illinois Institute of Technology, ANL-HEP-TR-97-57, (1996)
6. C. H. Ho, Ph.D. Thesis, UCLA, (1992)
7. E. Chojnacki, R. Konecny, M. Rosing and J. Simpson, Proceedings of the 1993 Particle Accelerator Conference, pg. 815 (Washington D.C., 1993)
8. *The Stanford Two-Mile Accelerator*, edited by R.B. Neal (W.A. Benjamin Inc., New York, 1968)
9. M. Menzel and H. Stokes, “User Guide for the POISSON/SUPERFISH Group of Codes”, Los Alamos National Laboratory Report No. LA-UR-87-115 (1987)
10. L.M. Young, Conference Proceedings of the Physics of Particle Accelerators, edited by M.Month and M. Dienes, AIP-184 (1989)

11. M. Reiser, *Theory and Design of Charged Particle Beams* (John Wiley & Sons, New York, 1994)
12. J.D. Lawson, *The Physics of Charged-Particle Beams, Second Edition* (Clarendon Press, Oxford, 1988)
12. Mathematica, computer software, Wolfram Research
13. J.G. Power, unpublished (1996)

LIST OF FIGURE CAPTIONS

FIG. 1. Variable delay laser system.

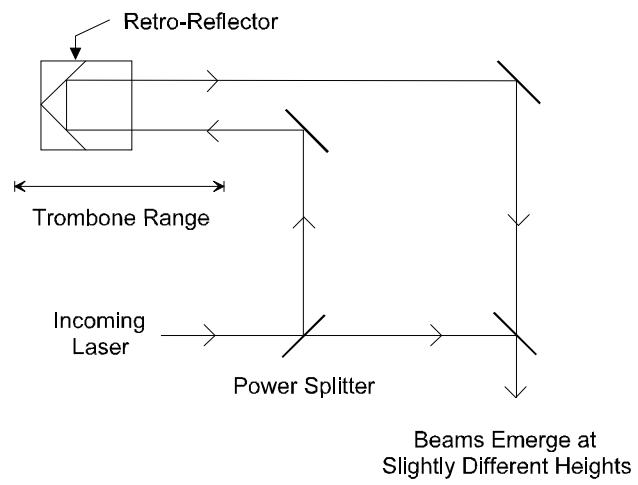
FIG. 2. Block diagram of the AWA facility.

FIG. 3. SUPERFISH simulation showing lines of constant r^*H_ϕ in the witness gun.

($a = 2.5$ cm, $b = 9.08$ cm)

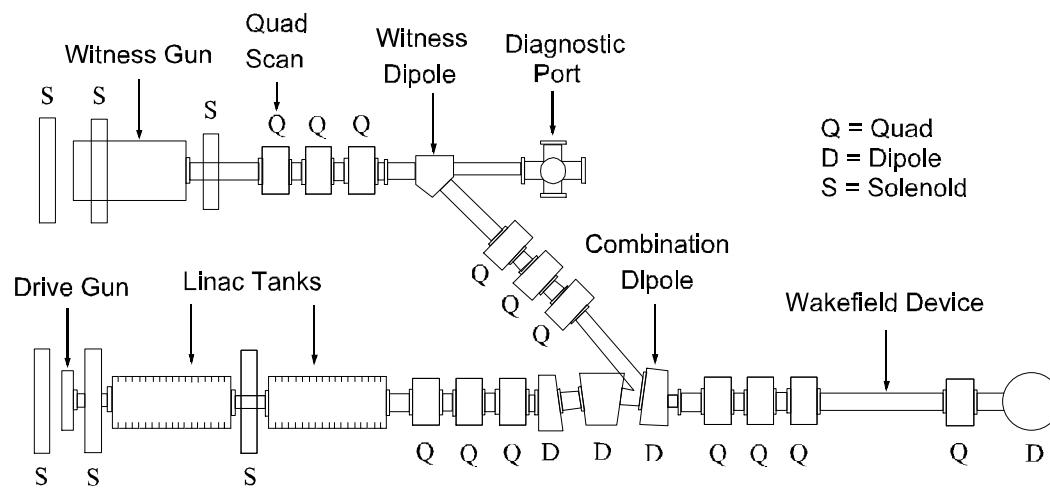
FIG. 4. Streak camera Image of the Witness Beam. $\Delta z = 11$ ps FWHM.

FIG. 5. Fit with space charge to the quad scan data for the witness beam.



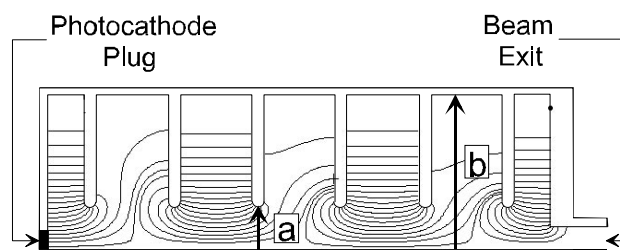
J. G. Power

FIG. 1. Variable delay laser system.



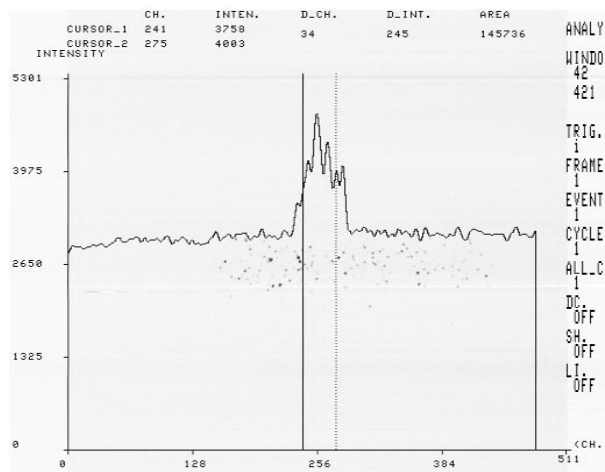
J. G. Power

FIG. 2. Block diagram of the AWA facility.



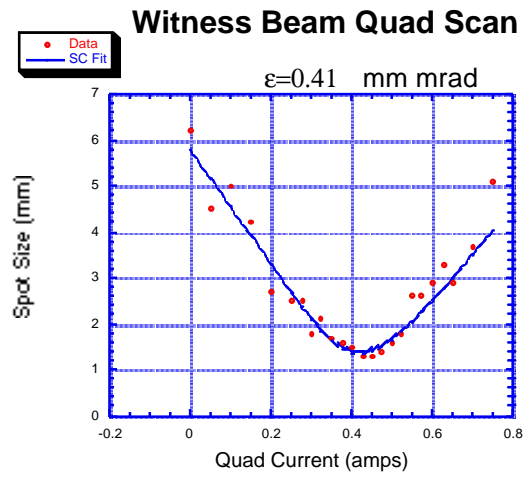
J. G. Power

FIG. 3. SUPERFISH simulation showing lines of constant r^*H_ϕ in the witness gun. ($a = 2.5$ cm, $b = 9.08$ cm)



J. G. Power

FIG. 4. Streak camera Image of the Witness Beam. $\Delta z = 11$
ps FWHM.



J. G. Power

FIG. 5. Fit with space charge to the quad scan data for the witness beam.